

Review

Evolution of purge with multi-sector, novel designs, and configurations of desiccant wheels: A technical review

*Évolution de la purge avec des configurations multi-sectorielles et des conceptions innovantes de roues déshydratantes : revue technique*

Laxmikant Yadav*, Ashutosh Kumar Verma

Department of Mechanical Engineering, National Institute of Technology Hamirpur, H.P., India

ARTICLE INFO

Keywords:

Novel design

Purge

Three and four sectors

Two-stage dehumidification

Mots clés:

Conception innovante

Purge

Trois et quatre secteurs

Déshumidification bi-étageée

ABSTRACT

This review provides a comprehensive summary of research pertaining to the purge section within desiccant wheels featuring multi-sector configurations. Additionally, it encompasses discussions on innovative wheel designs such as non-adiabatic desiccant wheels and the achievement of two-stage dehumidification from a single wheel employing multi-sector approaches. The review begins by providing a concise historical overview of the desiccant wheel, followed by a systematic classification of the research conducted in this area. Subsequently, various categorizations are presented in a logical sequence, offering a structured understanding of the subject matter. Central to the critical findings of this review is the identification of an optimal purge wheel sector angle, which not only decreases the energy consumption of the desiccant wheel but also significantly reduces the exit temperature of process air. Moreover, the review highlights the potential of achieving isothermal dehumidification through the utilization of non-adiabatic rotary desiccant wheels. Furthermore, the introduction of a multi-sector desiccant wheel is one of the key successes in obtaining two-stage dehumidification and getting multi-output like cooling, heating with dehumidification, and heating with humidification. These are all efficiently derived from a single wheel.

1. Introduction

Utilizing waste heat and energy from renewable sources is vital to the sustainable development of any Nation (Al-Shetwi, 2022; Seckin Salvarli and Salvarli, 2020). The renewable energy sector currently accounts for 26.53 % of India's overall installed generation capacity. To achieve 50 % renewable energy coverage for the country's energy demands by 2030, the Indian Ministry of New and Renewable Energy (MNRE) has put forth a proposal to install 500 GW of renewable energy systems (Ministry of New and Renewable Energy, 2010). As of 2021, the energy demand for the space cooling sector had the highest annual growth rate of any building end-use, accounting for nearly 16 % of the building sector's total electricity consumption (IEA, 2022). To reduce this energy consumption of space cooling, the researchers have successfully integrated a space cooling system with renewable sources, and they identified that a desiccant wheel-based HVAC system is one of the suitable alternatives to

the VCRS system for air dehumidification and air conditioning because it can be mainly operated by heat (thermal driven) or renewable source of energies (Jani et al., 2018; Dai et al., 2015; Beker et al., 2022; Kashif et al., 2020; Cerci and Hurdogan, 2022; Akhtar et al., 2024). A low-temperature heat source of approximately 60 to 90 °C is required as a main input for the regeneration (reactivation) of the rotary dehumidifier, and due to this exergy destruction can also be minimized in the regeneration process (Worek WM; K Choudhuri, 1982; Su et al., 2023; Dincer, 2007). However, in the conventional method (vapor compression method) of air dehumidification and air conditioning, electrical energy is used as the main input to run the system. In this method, the air is cooled below the condensation temperature of vapor, and dry air is produced. This leads to excessive cooling of air and increases the running cost of the system (Elsarrag et al., 2016; Chen et al., 2020; Robison, 1985). In addition, the refrigerant used in the system may cause environmental problems. These problems can be avoided using a desiccant wheel (DW), as the DW is especially popularized in lithium

* Corresponding author.

E-mail address: laxmikant@nith.ac.in (L. Yadav).

Nomenclature		<i>Subscript</i>
c_{pda}	Specific heat of dry air	Specific heat of dry air $\text{kJ kg}^{-1} \text{K}^{-1}$
c_{wr}	Reference specific heat	Reference specific heat $\text{kJ kg}^{-1} \text{K}^{-1}$
h	Heat transfer coefficient	Heat transfer coefficient $\text{W m}^{-2} \text{K}^{-1}$
\dot{m}	Mass flow rate	Mass flow rate kg h^{-1}
P1	Process section 1 for multi-sector wheel	Process section 1 for multi-sector wheel-
P2	Process section 2 for multi-sector wheel	Process section 2 for multi-sector wheel-
\dot{Q}	Heat	Heat W
R1	Regeneration section 1 for multi-sector wheel	Regeneration section 1 for multi-sector wheel-
R2	Regeneration section 2 for multi-sector wheel	Regeneration section 2 for multi-sector wheel-
T	Temperature	Temperature $^{\circ}\text{C}$
\bar{T}	Average temperature	Average temperature $^{\circ}\text{C}$
ttime	time	times
u	Velocity of air	Velocity of air m s^{-1}
\dot{V}	Discharge	Discharge $\text{m}^3 \text{h}^{-1}$
z	Axial direction of wheel	Axial direction of wheel-
<i>Greek symbol</i>		
α	Half of the height of the channel	Half of the height of the channel
ζ	Non dimensional length	Non dimensional length-
θ	Wheel sector angle	Wheel sector angle Degree ($^{\circ}$)
λ	Wall thickness	Wall thickness mm
ρ_{da}	Density of dry air	Density of dry air kg m^{-3}
ρ_w	Density of wheel	Density of wheel kg m^{-3}
τ	Non dimensional time	Non dimensional time-
ω	Humidity ratio	Humidity ratio kg kg^{-1}
$\bar{\omega}$	Average humidity ratio	Average humidity ratio kg kg^{-1}
<i>Abbreviation</i>		
AH	Air heater	
CHE	Cross flow heat exchanger	
COP	Coefficient of performance	
CV	Control volume	
DCHE	Desiccant coated heat exchanger	
DCOP	Dehumidification Coefficient of Performance	
DEC	Direct evaporative cooling	
DW	Desiccant wheel	
EER	Energy efficiency ratio	
GSR	Gas side resistance	
GSSR	Gas and solid side resistance	
HE	Heat Exchanger	
HVAC	Heating, ventilation, and air conditioning	
ICDW	Internally cooled desiccant wheel	
MNRE	Ministry of New and Renewable Energy	
MOF	Metal-organic framework	
MR	Moisture removal	
MRC	Moisture removal capacity	
MRR	Moisture removal rate	
RH	Relative humidity	
RMR	Relative moisture removal	
rph	Revolution per hour	
TSDSW	Two-stage dehumidification from a single wheel	
TSDTW	Two-stage dehumidification from two-wheel	
VCRS	Vapour compression refrigeration system	
WHR	Waste heat recovery	

battery manufacturing, cold stores, data centers, and pharmaceutical sectors to produce a very low level of indoor humidity (less than 0.3 g kg^{-1}) continuously (Ma et al., 2024; Yin and Yin, 2021; Zhang et al., 2024; Chen et al., 2019). Further, researchers have successfully integrated the desiccant wheel with evaporating cooling & heat pump and vapor compression system to handle the latent load of building separately and achieved air conditioning using waste heat (condenser waste heat) or solar heat (Abdelgaiad et al., 2023; Tian et al., 2022; Yang et al., 2024; El-Agouz and Kabeel, 2014; Angrisani et al., 2016; Mohammed et al., 2023). However, these desiccant wheels are generally two-sector desiccant wheels. Because the DW is a critical component of any air dehumidification or solid desiccant air conditioning unit it must be properly installed, (Farooq and Ruthven, 1991; Ebrahimi and Keshavarz, 2015).

Thus, by modifying the designs and configurations of the rotary dehumidifier, the overall system's performance can be enhanced, and further development is possible on the purge concept and new designs and configurations of the desiccant wheel so that it can be utilized in a variety of applications. Therefore, it is imperative to condense these concepts into a review format to facilitate researchers' engagement with these ideas.

A review on dehumidification was presented by Mazzei et al. (2005), they carried out a review on the dehumidification process for HVAC and pointed out that desiccant wheel-based dehumidification provides better control of moisture with less running cost than the mechanical based dehumidification. The article provides a categorization of desiccant wheel systems, specifically focusing on two areas: (i) an evaluation of desiccant wheel-based HVAC, and (ii) an assessment of the technical

advancements in desiccant wheel technology.

The review of the first category was initiated by Daou et al. (2006). They reviewed desiccant air conditioning systems and concluded that the main attractive feature of desiccant systems is that they can be regenerated by low-temperature energy sources or waste heat. Again, a review of the desiccant wheel-based cooling systems was written by Ge et al. (2014) and Sultan et al. (2015), but the focus of this review was on the distinct solar-powered system and hybrid solar-powered single and double-stage systems. Further, Mujahid Rafique et al. (2015) have done a detailed review of the desiccant-based evaporative air conditioning system, which is available in the literature, and reported that an evaporative cooler integrated with a desiccant wheel system can provide thermal comfort in hot and humid weather. Jani et al. (2016) carried out an exhaustive literature survey on desiccant cooling. They summarized the different desiccant cooling cycles operated in different modes, mathematical modeling of the DW, solar and hybrid desiccant cooling systems, etc. in a single review article.

Similarly, the review of the second category was initiated (Ge et al., 2008b), they presented a detailed review of the mathematical modeling of the DW to explore the overall performance of the dehumidifier. In this review, they presented the different types of mathematical models developed by researchers and indicated that the GSSR (gas and solid side resistance) model is more accurate and complicated than the GSR (gas side resistance) model. The GSSR model was created by Ge et al. (2010c) to analyze the performance of a novel compound silica gel haloid desiccant wheels under various operating conditions, and it has since been widely used by other researchers. La et al. (2010) carried out a technical review on advanced desiccant materials and optimum

configurations of the rotary dehumidifier system. Rambhad et al. (2016) summarized the different dehumidification and regeneration methods of solid desiccants and concluded that desiccant wheel systems have lower running and maintenance costs and are better for the environment. Wu et al. (2018) conducted a literature review on the substrate (matrix) material of the DW and found that glass fiber or ceramic fiber paper is commonly employed as the substrate for the rotary dehumidifier. In this study, they indicated that substrates with higher thermal conductivity and higher porosity were desirable for better dehumidification effectiveness of the desiccant wheel. Shamim et al. (2021) summarized the work of solid desiccant dehumidifiers from the perspective of net zero energy building. In this article, they talked about novel desiccant materials, innovative designs of wheels, and different regeneration methods of solid desiccants.

A key limitation of solid desiccant dehumidification is the heat released during adsorption due to capillary condensation, which raises the supply air temperature. To address this, the desiccant coated heat exchanger (DCHE) was introduced in (Ge et al., 2010a), coating desiccants on heat exchanger fins to achieve high energy efficiency. Feng et al. (2022) reviewed DCHE, providing a comprehensive understanding of the technology. Their review facilitates further research, design improvements, and optimization, and identifies potential applications like humidity pumps, water harvesting, and thermal management.

Recently, Abd-Elhady et al. (2022) reviewed in depth the various configurations and methods of solid desiccants, including packed beds, fluidized beds, and rotary dehumidifiers. In this study also, they talked about the development of different configurations and new designs of desiccant wheels.

As previously stated, the researchers presented several review articles. Nevertheless, to the best of the author's knowledge, there has been no scholarly article that examines novel wheel designs, desiccant wheels with multiple sectors, two-stage dehumidification using a single wheel, or desiccant wheel configurations in a single publication. As a result, the goal of this review is to present these aspects of a desiccant wheel effectively so that researchers can conduct additional research in these areas and contribute to the progress of novel desiccant wheel designs for the benefit of society.

2. Brief history and categorization of work done till now

2.1. Brief history of the desiccant wheel

Desiccant materials have been used in US industries since 1930 to control humidity (Mei et al., 1992) and in desiccant cooling (Pesaran et al., 1992). The potential of desiccants was also identified by Munters (2022) and he developed the first rotary dehumidifier (desiccant wheel) for cold storage rooms in 1951. After that in 1955, the aluminum wool pad with poly-ethylene glycol-based rotary dehumidifier was introduced

by Pennington (1955) and got a patent for the cooling cycle, also called the Pennington cycle or ventilation cycle. Further, in the mid-1960s, (Dunkle, 1965) proposed a method for solar air conditioning using a rotary dehumidifier. With the progress of technology, Muter introduced a parallel passage in the desiccant wheel and reduced pressure drop (Munter, 1968). But this wheel was granular bed type and not properly airproof. To overcome this, considerable effort has been made by researchers to prevent the leak of air from the process of regeneration. Thereafter, researchers proposed a honeycomb-type desiccant wheel, and the focus was to improve lifetime and reduce cost. They improved the durability by replacing LiCl with silica gel as a desiccant. At that time, desiccant systems were used for drying the air, but the potential to use these systems was more recognized in comfort-related areas like supermarkets (Mei et al., 1992).

2.2. Categorization of work done on a desiccant wheel

As shown in Fig. 1, the work done on the various aspects of a rotary dehumidifier can be broadly classified into three categories. In the first category, numerous mathematical and experimental studies (Ge et al., 2010c; De Antonellis et al., 2010; Yadav and Bajpai, 2012; Angrisani et al., 2012; Ahmed et al., 2005; Yadav and Yadav, 2018a; Intini et al., 2015; Vivekh et al., 2023; Motaghian et al., 2021), including those utilizing ANN methods, have been carried out. Researchers have provided the optimal values of these parameters, as shown in Table 1. Similarly, in the second category, research on various advanced desiccants and composite desiccants (Wu et al., 2018; Majumdar, 1998; Zhang et al., 2014; Liu et al., 2022; Bharathi et al., 2023; Zhang et al., 2024; Xue et al., 2024; Chung et al., 2023) with different substrate materials is presented, with a summary of some of these studies shown in Table 2. The third category is related to the purge, novel configurations, and new designs of the desiccant wheel (Abd-Elhady et al., 2022).

3. Innovative designs and configurations of a desiccant wheel

The innovative design and configurations of a desiccant wheel can be categorized into three main categories and further divided into sub-categories as shown in Fig. 2 which are discussed in detail way in the subsequent sections.

3.1. Evolution of purge with three and four-sector desiccant wheel

The evolution of purge started in the mid-70 s to reduce the carry-over (ASHRAE, 1974). The carryover problem was more prominent in industries because air-to-air rotary heat exchanger was widely used to utilize the waste heat of the exhaust stream in the process stream (Herath et al., 2020). As the wheel rotates from the exhaust stream to the process streams of air, some exhaust particles (contaminants) of the

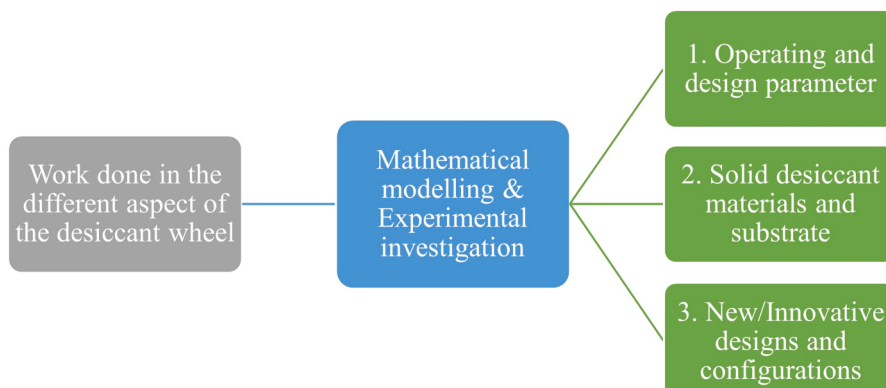


Fig. 1. Work carried out on a desiccant wheel.

Table 1

Summary of work carried out on operating and design parameters of DW.

Reference	Methodology	Optimum operating parameter	Optimum design parameter
(Ge et al., 2010c)	Simulation	Regeneration temperature: 80 °C - 95 °C The process air flow rate: 2- 3.5 m s ⁻¹ Regeneration air flow rate: 2.5-3.5 m s ⁻¹	Regeneration wheel sector angle: 100°–160°
(De Antonellis et al., 2010)	Simulation	-	Process wheel sector angle: 200° for maximum MRC 260° for minimum heat of regeneration Wheel length: 0.2 m Process to regeneration area ratio: 0.7–0.8 Aspect ratio: 0.3–0.5 Channel pitch: 0.003–0.005 m Channel height: 0.002–0.004 m Wheel porosity: 0.4–0.6
(Yadav and Bajpai, 2012)	Simulation	-	
(Angrisani et al., 2012)	Experimental	Dehumidification effectiveness: 0.43 for $u_r/u_p = 0.5$ 0.54 for $u_r/u_p = 1$ Moisture removal capacity: 2.5–3.7 kg h ⁻¹	-
(Ahmed et al., 2005)	Simulation	-	Wheel thickness: 0.26 m for 60 °C T_r and 0.18 m for 90 °C T_r Regeneration fraction area: 0.8 for 60 °C T_r and 0.3 for 90 °C T_r Wheel porosity: 0.4–0.7
(Yadav and Yadav, 2018a)	Simulation	Rotational speed: 20 rph Regeneration Temperature: 60 °C Process velocity: 2 m s ⁻¹ Regeneration velocity: 2 m s ⁻¹	For a lower sensible energy ratio; Wheel length: 10 cm Wall thickness: 0.2 mm Channel pitch: 3 mm Channel height: 5 mm
(Intini et al., 2015)	Experimental and numerical simulation	Revolution speed 10 rph –50 rph when the area ratio is 0.5 to 0.8 and regeneration temperature between 60 and 120 °C	Process to total cross-section area ratio: 0.5

exhaust stream are adsorbed on the wheel matrix, and when it encounters process air, the adsorbed particle mixes into the process air and goes to the supply side as shown in Fig. 3(a) (DAC, 2022). But when a small purge section is placed in the DW, the carryover particle is rerouted towards the regeneration stream due to pressure difference as shown in Fig. 3(b). According to reference (ASHRAE, 1974), carryover impurities (contaminants) can be decreased to less than 0.1 % of the exhaust streams by installing a purge section in a rotary heat exchanger.

At the end of the 80 s, the idea of a purge section in a rotary dehumidifier was introduced by San (1988) to prevent cross contamination as in the case of a heat wheel. In addition, the second objective was to cool

Table 2

Summary of work carried out on DW made of different materials and substrate.

Reference	Desiccant material and substrate used	Key finding
(Majumdar, 1998)	Composite of silica gel desiccant and inert material (fiber)	When the capacitance ratio was 8 or higher, the cooling capacity reached its peak at a volume fraction (inert material) = 0.2. The ability to cool increased by 19.5 % with a thermal capacitance ratio of 24.
(Intini et al., 2015)	Synthetic Zeolite AQSOA-based desiccant	The best uses for this zeolite material were at medium and high temperatures, with a regeneration temperature of between 80 °C and 100 °C. The area ratio had a big effect on the optimal revolution speed. A higher area ratio led to a faster optimal revolution speed.
(Zhang et al., 2014)	Honeycomb type adsorbent	Silica gel 3A and silica gel RD exhibited superior dehumidification capabilities compared to alternative desiccants when utilized in typical operational circumstances and equipped with low-grade waste heat.
(Liu et al., 2022)	Metal-organic framework composite adsorbent desiccant wheel	The temperature increase at the inlet and outlet of this wheel was comparatively lower than that of a standard wheel when the ambient humidity ratio was low. Conversely, when the ambient humidity ratio was high, the opposite occurred. The performance coefficient and capability of the MOF DW to remove moisture from the air increased by 40 %–48 % and 13 %–19 %, respectively.
(Bharathi et al., 2023)	Glass fiber, ceramic fiber, nomex fiber, and brown wood pulp substrates coated with nano SiO ₂	As the desiccant coatings got thicker, the ability to soak up water got better. With a value of 57.6 g m ⁻² , the Glass fiber paper-SiO ₂ desiccant wheel could hold a lot of water. At 50 °C, the Glass fiber paper-SiO ₂ desiccant wheel had a higher dehumidifying capacity of 2.1 kg ⁻¹ and a dehumidifying coefficient of performance of 2.2.

the hot desiccant matrix when it came from the regeneration stream. San carried out the analysis of the desiccant-based air conditioning system in ventilation mode at different fractions of the purging section and found that the optimum value of this fraction was 6 % for maximum cooling capacity. After that Harshe et al. (2005) made a two-dimensional steady numerical heat and mass transfer model for the analysis of the rotary dehumidifier of three sections, namely, regeneration, process, and purge. However, the experimental analysis of the purge sector (third sector) desiccant wheel was proposed by Nagaya et al. (2006) for food drying, they called this area a heat collection zone as shown in Fig. 4(a). This third zone ($\theta_{pg} = 90^\circ$) was utilized to release the carryover heat into the fresh air, then this preheated air was heated by a heater and diverted to the regeneration section. Thus, obtained a 6 times faster drying rate than the usual desiccant-operated drying.

However more focused research on purge was started by Golubovic et al. (2007), and they built a mathematical model to analyze the impact of purge wheel sector angle in a detailed way. Their primary findings indicate that as the wheel transitioned from regeneration to the process side, the exit humidity ratio of the process air decreased during the beginning of the adsorption sector, reaching its minimum value at a

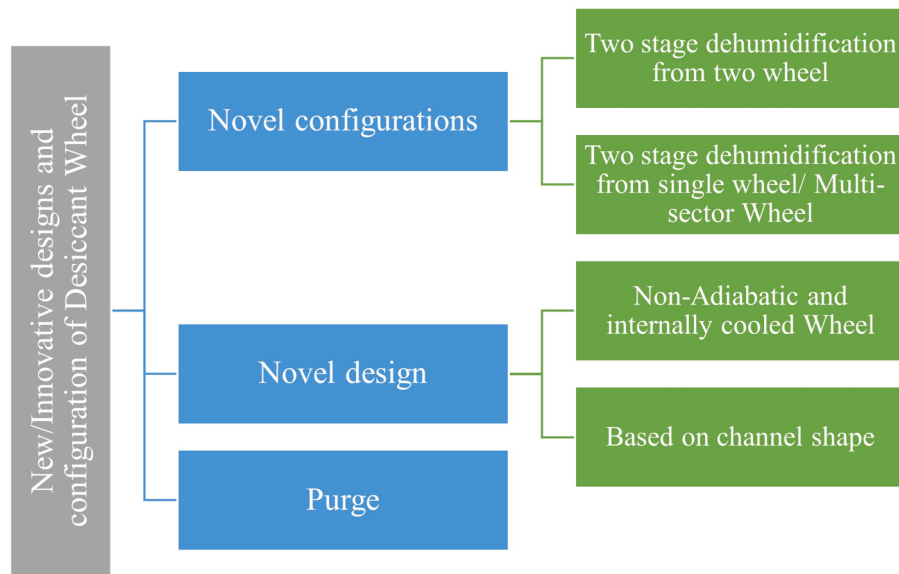


Fig. 2. Innovative design and configuration of the desiccant wheel.

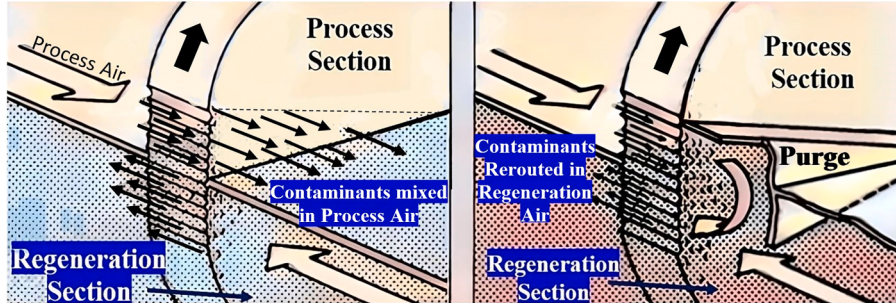


Fig. 3. (a) without purge, (b) with purge (DAC, 2022).

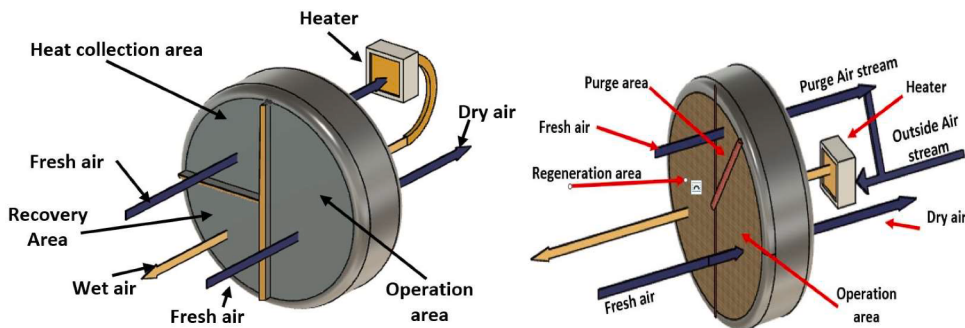


Fig. 4. (a) Desiccant rotor with heat collection zone (Nagaya et al., 2006), (b) Purge outlet utilized for regeneration (Golubovic et al., 2007).

specific adsorption wheel sector angle as illustrated in Fig. 5, termed the effective purge wheel sector angle. After this, the exit humidity ratio is almost constant in remaining adsorption wheel sector angles. Therefore, they isolated this starting segment of the adsorption stream up to the effective purge wheel sector angle, where humidity ratio decreases to its minimum value, from the rest of the adsorption stream, naming it the purge stream. They observed that this purge stream had a higher exit temperature compared to the remaining process stream and utilized this warmer stream for regeneration, as illustrated in Fig. 4(b). Thus, saved some regeneration energy. Further, Table 3 presents results for two non-dimensional lengths (5 & 20) and their corresponding non-dimensional times, both with and without the application of a

heated purge (Golubovic et al., 2007). From this table, it is seen that the exit humidity ratio of process air ($\omega_{p,out}$) with purge is 30 to 59 % lower than $\omega_{p,out}$ of the same wheel having no purge. Likewise, the outlet processes air temperature ($T_{p,out}$) with purge is 3 to 7 °C lower than the $T_{p,out}$ of the same wheel having no purge. Further, the average effective purge wheel sector angle was 28–30° at 170 °C and increased to 38–40° when the regeneration temperature decreased to 140 °C. The non dimensional length (τ) and non-dimensional time (ζ) are defined in Eq. (1) (Golubovic et al., 2007):

$$\tau = \frac{h}{\rho_w \lambda c_{wr}} t \text{ and } \zeta = \frac{h}{\rho_{da} u \alpha c_{pda}} z \quad (1)$$

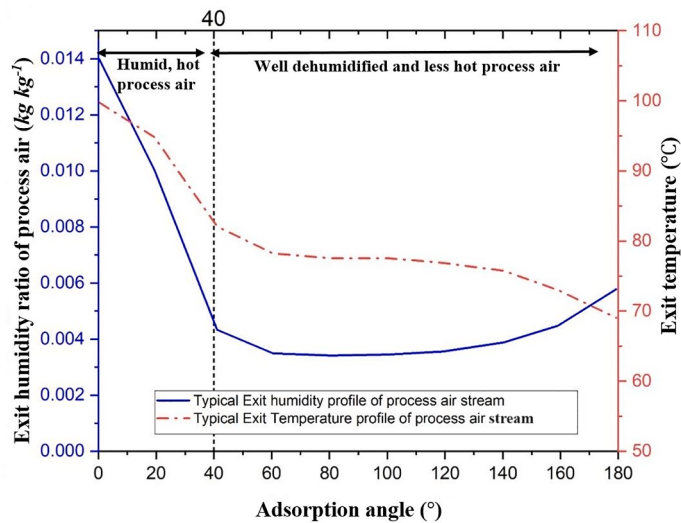


Fig. 5. Effect of adsorption wheel sector angle on exit humidity ratio and exit temperature of process air stream (Golubovic et al., 2007).

Table 3

$\omega_{p,out}$ and $T_{p,out}$ for two cases of nondimensional length and time (Golubovic et al., 2007).

Regeneration temperature = 140°C			
Nondimensional length = 5		Nondimensional length = 20	
Optimum non dimensional time = 48		Optimum non dimensional time = 260	
Purge wheel sector angle (°)	0	37.8	0
$\omega_{p,out}$ (kg kg^{-1})	0.00353	0.00246	0.00206
$T_{p,out}$ (°C)	85.8	78.9 °C	88.6 °C
			82.1 °C

In addition to carryover, the other benefits of a purge section according to the results of the literature (Golubovic et al., 2007) are presented below:

- It reduces the temperature of the desiccant matrix when the wheel rotates from a hotter regeneration stream to a colder process stream, thereby less carryover heat goes to the process section, and that enhances the dehumidification performance by lowering the exit humidity ratio.
- As it reduces the desiccant matrix temperature, it becomes hotter by taking heat from the hot matrix and if it is diverted toward the regeneration section, it can reduce the regeneration energy of the DW.
- The reduction in carryover heat not only facilitated post-cooling subsequent to dehumidification but also diminished the consumption of regeneration energy of the rotary dehumidifier.

The only negative impact is that it reduces the mass flow rate of the process stream by a reduction in process area (Golubovic et al., 2007). The significance of purge on the performance of the enthalpy wheel was again discussed by Zhai et al. (2009) and Ruan et al. (2012) and they simulated that the required purge wheel sector angle was 11°. They found that the area of the purge sector depends upon wheel length (depth), purge airflow, and rotational speed of the rotary dehumidifier. An increase in wheel length and rotational speed from the optimum value required more purge air to avoid carryover leakage, thus decreasing the performance of the enthalpy wheel (Ruan et al., 2012). The inclusion of purge reduced the cross-contamination, but from the result of (Zhai et al., 2009), it was also reflected that the introduction of purge wheel sector angle reduced the performance by 5 % for the enthalpy wheel.

Yadav and Bajpai (2012) formed a numerical heat and mass transfer model to study the performance of new designs of a DW which having two purge sections, namely, cooled purge (purge 1) and heated purge (purge 2) as shown below in Fig. 6(a). Since the output of purge 2 has been used to preheat the desiccant matrix in purge 1 and the output of purge 1 has been used to precool the desiccant matrix just after the regeneration. Thus, these two purges transmit their heat mutually and enhance the performances in the higher ranges of regeneration temperatures (90 °C) of that study (Yadav and Bajpai, 2012). Hence, it can be concluded that the inclusion of heated and cooled purges and their mutual utilization of heat can be beneficial when the rotary dehumidifier is regenerated from a higher temperature of the air. The same mathematical model has been further used by Yadav (2014), Yadav and Yadav (2014) to study the behavior of the DW when the output of the purge became an input of the regeneration stream according to reference (Golubovic et al., 2007). In addition, Yadav (2014) also carried out the comparative analysis between the clockwise and anti-clockwise rotation of the DW with purge (shown in Fig. 6(b) and (c)) and found that anticlockwise spin of the wheel yields superior RMR efficiency in all considered cases. The main difference in references (Golubovic et al., 2007; Yadav, 2014; Yadav and Yadav, 2014) is the magnitude of the purge wheel sector angle. In (Golubovic et al., 2007) variation of the purge wheel sector angle was studied and determined effective purge wheel sector angle, but in (Yadav and Yadav, 2014) purge and regeneration wheel sector angles were fixed at 90° like reference (Nagaya et al., 2006). Since the taken purge wheel sector angle was far greater than the optimal value, the RMR efficiency of anticlockwise rotation was better than the clockwise. Furthermore, because of the higher purge wheel sector angle air got slightly dehumidified and heated which can be utilized in the regeneration section. This concept was used in reference (Yadav and Yadav, 2014), where they referred to the regenerative sector as an effective regeneration sector and compared it to the conventional (ordinary) regeneration sector when simple hot air was supplied to regeneration without the use of purge output as shown in Fig. 6(d) and (e) (Yadav and Yadav, 2014). Thus, the consumption of regeneration energy was reduced and the regeneration effectiveness of a DW with an effective regeneration sector was improved in comparison to ordinary regeneration sectors. Like the effective regeneration sector (Yadav and Yadav, 2014), an effective adsorption sector was also introduced by Yadav and Yadav (2015), where the output of purge was passed into the process section and comparative analysis between the effective adsorption sector and effective regenerative sector were carried out using the same model. But in this case, the process of purge and regeneration were equally divided as depicted in Fig. 7(a) and (b). The

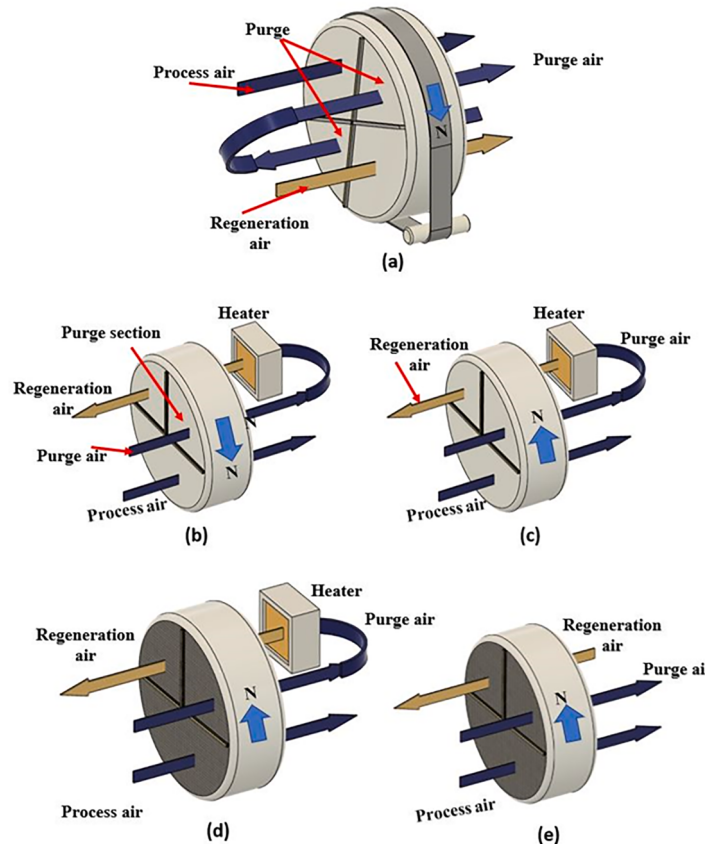


Fig. 6. (a) to 6(e). Novel configurations of purge-I (Yadav, A. and Bajpai, 2013, 2014; Yadav and Yadav, 2014).

main reason to introduce an effective adsorption sector was to achieve two-stage dehumidification from a single wheel because some dehumidification occurs in the purge also due to the larger area. But total dehumidification was lesser than the effective regeneration sector wheel. Because pre-dried and warm air was supplied to the regeneration section which enhanced the regeneration performance but when the same air was supplied to the adsorption section, less adsorption was achieved in the second stage since comparatively less moisture was present in the output of the purge stream.

Yadav and Yadav (2016) made a math model to analyze the impact of the purge wheel sector angle when the DW rotates either clockwise or anticlockwise. They put a small purge sector in the regeneration section of the DW. When the wheel rotated anticlockwise, the purge was at the end of the regeneration section, but when it rotated clockwise, it was at the end of the process section, as shown in Fig. 7(c) and (d). The effect of purge wheel sector angle between 5 and 20° had been studied and determined its optimal value for different operating conditions in both directions of rotation. Their findings indicated that for given cases, the anticlockwise direction of the wheel performed slightly better than the clockwise direction of rotation, but the influence of change in purge wheel sector angle was slightly greater in the clockwise direction compared to the anticlockwise direction. In the study (Yadav and Yadav, 2016), the purge was placed arbitrarily on the regeneration side, but this can also be installed on the process side. So, to investigate the position of this sector (Yadav and Yadav, 2018b) used the same model and introduced three arrangements of the wheel based on the position of a purge. In the first arrangement, TSS was installed on the process side but in the second it was placed on the process side, and in the third arrangement, the position of the purge was in such a way that it occupied an equal area in both the process and regeneration section as shown in Fig. 7(e), (f) and (g). Yadav and Yadav (2018b) carried out a comparative study of these arrangements and found that a purge should be installed on the

process side when moisture removal is the main concern. On the other hand, when lower exit temperature and moderate moisture removal are the primary requirements, then it should be installed on the regeneration side.

As Golubovic et al. (2007) pointed out the mass flow rate in the process section decreases when an effective purge wheel sector angle is incorporated into the desiccant wheel. To solve this issue, Mandegari et al. (2017) presented the concept of optimal purge wheel sector angle which was different from the concept of effective purge wheel sector angle as introduced in (Golubovic et al., 2007). The optimal purge wheel sector angle was defined as the maximum difference between the purge and process sectors' average humidity ratios, as shown in Eq. (2) (Mandegari et al., 2017).

$$[\theta_{pg}]_{optimal} = \text{maximum}[\bar{\omega}_{pg,out} - \bar{\omega}_{p,out}] \quad (2)$$

To carry out the overall investigation, the researcher Mandegari et al. (2017) established a two-dimensional heat and mass transfer model to analyze the influence of operating (process and regeneration velocities, rotational speed, and reactivation temperature) and design parameters (wheel length, channel thickness, channel hydraulic diameter) on required wheel sector angles (effective and optimal) and obtained some results which are indicated in Table 4. From this table, it can be noticed that in the case of no purge, the flow rate in the process section was 340 $m^3 h^{-1}$ and average exit humidity ratio of process air ($\bar{\omega}_{p,out}$) was 0.0031 $kg kg^{-1}$. On the other hand, in the case of an effective purge wheel sector angle, a significant fraction (74%) of process air exited from the wheel as purge air, and the flow rate of the remaining process air was reduced from 340 to 246 $m^3 h^{-1}$ but $\bar{\omega}_{p,out}$ decreased from 0.031 to 0.0021 $kg kg^{-1}$ as indicated in Table 4. So, to get the same mass flow rate as when there was no purge, a bigger DW was needed, which led to higher costs at the start and over time. According to the above definition, the optimal purge wheel sector angle was 12° (6 s) which is significantly

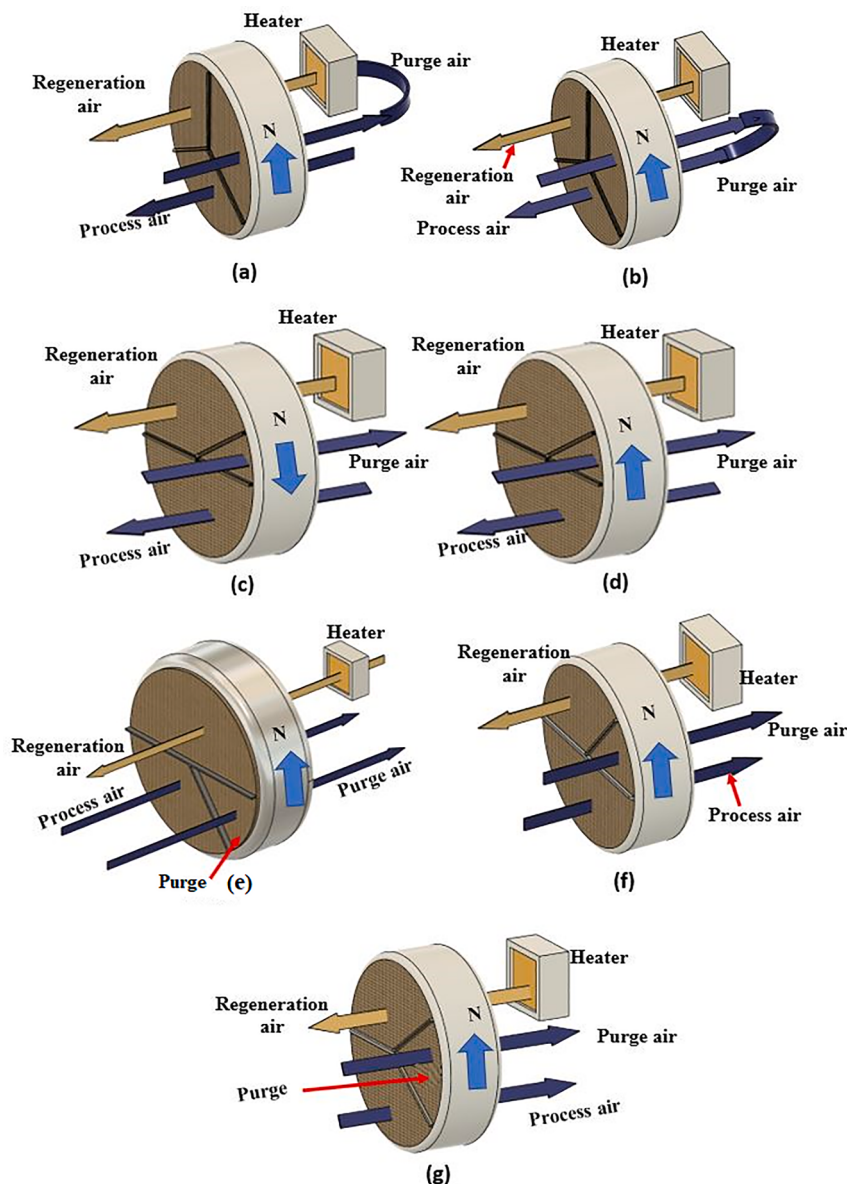


Fig. 7. (a) to 7(g). Novel configurations of purge-II (Yadav and Yadav, 2015, 2016, 2018b).

lower than the effective purge wheel sector angle of 74° (37 s). Due to this flow rate was increased in the process section from $246 \text{ m}^3 \text{ h}^{-1}$ to $324 \text{ m}^3 \text{ h}^{-1}$ but lower than with no purge. Thus, the moisture removal rate (MRR) of a DW with optimal purge was greater than the effective purge and with no purge, because MRR is the combined effect $\bar{\omega}_{p,out}$ and flow rate. Furthermore, the required regeneration heat and dehumidification coefficient of performance (DCOP) were better with optimal purge, as indicated in Table 4. The DCOP value represents the overall effect of dehumidification and energy efficiency, defined as the ratio of the latent heat of adsorbed water to the required regeneration heat.

Recently, Motaghian and Pasdarshahri (2020) determined the purge wheel sector angle based on the minimum moisture content of process air and called this angle an effective purge wheel sector angle. In addition, the purge wheel sector angle determined, based on the maximum COP of the desiccant wheel was called as optimal purge wheel sector angle. However, they pointed out that the determination of purge wheel sector angle based on maximum COP was a better criterion than the minimum humidity ratio because COP combined the effect of moisture removal, mass flow rate, and regeneration energy. Their results indicated that the value of optimum purge wheel sector angles was 37 to

68 % wider than the corresponding effective purge wheel sector angles for investigated configurations. Furthermore, the % saving in regeneration energy in the case of optimal purge wheel sector angle was also 10–11 % greater than the case of effective purge wheel sector angle.

3.2. Novel configurations

In novel configurations, two-stage dehumidification from DW has been covered. The two-stage dehumidification can be broadly categorized into two categories: (i) Two-stage dehumidification from two-wheel (TSDTW) with two sectors, (ii) Two-stage dehumidification from the single wheel (TSDSW) with multi sectors:

3.2.1. Two-stage dehumidification from two wheels (TSDTW) with two sectors

There are many research articles available with two-stage dehumidification from two wheels. The two-stage dehumidification from two desiccant wheels (TSDTW) was initiated by Ge et al. (2009). In this work, they experimentally investigated the performance of TSDTW at several operating variables. The proposed system is depicted in Fig. 8, it

Table 4

Comparison of optimal purge with effective purge and no purge (for inlet humidity, ratio, $\omega_{p,in} = \omega_{pg,in} = 0.015 \text{ kg kg}^{-1}$) (Mandegari et al., 2017).

Parameters	Symbol	Without purge	Effective purge	Optimal purge
Purge parameters	θ_{pg}	—	74°	12°
	$\bar{\omega}_{pg,out}$	—	0.0056 kg kg^{-1}	0.010 kg kg^{-1}
	$\bar{T}_{pg,out}$	—	81.8 °C	98.3 °C
	\dot{V}_{pg}	0	94 $\text{m}^3 \text{ h}^{-1}$	16 $\text{m}^3 \text{ h}^{-1}$
	\dot{m}_{pg}	0	109.41 kg h^{-1}	18.62 kg h^{-1}
Process parameters	$\bar{\omega}_{p,out}$	0.0031 kg kg^{-1}	0.0021 kg kg^{-1}	0.0027 kg kg^{-1}
	$\bar{T}_{p,out}$	63.4 °C	56.5°C	61.8 °C
	\dot{V}_p	340 $\text{m}^3 \text{ h}^{-1}$	246 $\text{m}^3 \text{ h}^{-1}$	324 $\text{m}^3 \text{ h}^{-1}$
	\dot{m}_p	395.76 kg h^{-1}	286.34 kg h^{-1}	377.13 kg h^{-1}
Wheel parameters	MRR	2.99 kg h^{-1}	2.48 kg h^{-1}	3.01 kg h^{-1}
	Q_r	4.01 kW	3.10 kW	3.76 kW
	DCOP	0.4691	0.5033	0.5036

was noticed that process air was passed over the first rotary dehumidifier where it became warm and dry. This warm air was cooled in the 1st sensible heat exchanger and then delivered to the second rotary dehumidifier for second-stage dehumidification. The resulting air from the second stage was again supplied to a second heat exchanger for further cooling. The cooling effect in both the heat exchangers was produced by supplying the air from the evaporative cooler. After that, this air was supplied to both heaters for the regeneration of both wheels as shown in Fig. 8.

The main finding of this research was that the reactivation temperature needed for regeneration was lower than the single-stage dehumidification system. Similarly, (Ge et al., 2010b; La et al., 2011; Li et al., 2012; Tu et al., 2014; Ge et al., 2015; Tavakol and Behbahaninia, 2018; Asadi and Roshanzadeh, 2019) have carried out detailed research on two-stage dehumidification using two desiccant wheels as shown in Table 5. However, the objective of this review is to discuss the details of only one rotor system. Hence, two-stage dehumidification with two wheels is not described in detail.

3.2.2. TSDSW with multi-sectors

The main cause of introducing two-stage dehumidification from a single wheel is to reduce the weight of the rotary dehumidifier and to obtain more new configurations of the desiccant wheel. The TSDSW was achieved by references (Yadav and Yadav, 2016; Ge et al., 2008a; La et al., 2012; Zeng et al., 2014; Verma et al., 2022) in a multi-sector desiccant wheel. They split the desiccant wheel into four sections of wheel sector angles P1 = 135°, P2 = 135°, R1 = 45°, and R2 = 45° as shown in Fig. 9. The desiccant wheel with three sections (process, regeneration, and purge) has been already described in the previous section. In this research, the process air was sent to the first process

section (P1) where dehumidification of air takes place. During this carryover heat and adsorption heat raised the process air temperature. Due to this, the resulting air was cooled in a sensible heat cooler and then supplied to the P2 section for second-stage dehumidification. Similarly, regeneration was achieved by heating the mixture of room return air and outdoor air. An investigation was conducted to assess the performance of this system under various operating conditions. The findings indicate that TSDSW is a viable option, offering comparable performance to TSDTW (two-stage dehumidification from two-wheel). Additionally, TSDSW is significantly smaller in size, approximately half the size of TSDTW.

The development of TSDSW was again introduced by Jeong et al. (2010). They integrated VCRS systems (three evaporators and three condensers) and the four-partition desiccant wheel to obtain two-stage dehumidification, air conditioning, and regeneration from a low-temperature heat source as shown in Fig. 10. The overall functioning of the system was analyzed at different reactivation temperatures, process air temperature, and rotational speed and it was found that the COP of this system was 94 % greater than the conventional VCRS system.

Further, the novel concept of two-stage dehumidification with a six-sector desiccant wheel (Fig. 11) was introduced by Elzahzby et al. (2014). In this work, the wheel had two processes, two regeneration, and two cooling sections. The cooling sections were installed just after the regeneration sections to neutralize the carryover heat and heat of adsorption. The performance of this six-sector desiccant wheel was analyzed under varying operating and design conditions by developing a numerical model, and their results reported that the optimal value of regeneration temperature, regeneration velocity, and area ratio (area of process section to regeneration section) were 90 °C, 2.5 m s^{-1} and 2.2, respectively.

The current challenge in researching one-rotor multi-sector desiccant wheels or TSDSW lies in their complexity. Unlike two-sector wheels, which only require two ducts for process and regeneration air, three- or four-sector wheels demand three or four ducts for process, regeneration and purge air streams, leading to heightened system complexity and costs. While sealing of air may present an issue, modern sealing techniques, coupled with strategic fan installation, for different air streams effectively mitigate this concern in multi-zone wheels. Moreover, dividing the wheel into more than four sectors introduces practical difficulties and operational challenges. Beyond this point, maintenance and system complexity become increasingly problematic. Therefore, while multi-sector desiccant wheels offer benefits, practical constraints limit the feasibility of further division.

3.3. Novel designs (Non-adiabatic and internally cooled desiccant wheel)

When atmospheric air passes through the adsorption section of the rotary dehumidifier, it dehumidifies and becomes warmer as a result of the carryover heat of regeneration and the heat of adsorption. This heat raises the temperature of the desiccant surface and reduces the adsorption capacity of the wheel. In the case of an air conditioning

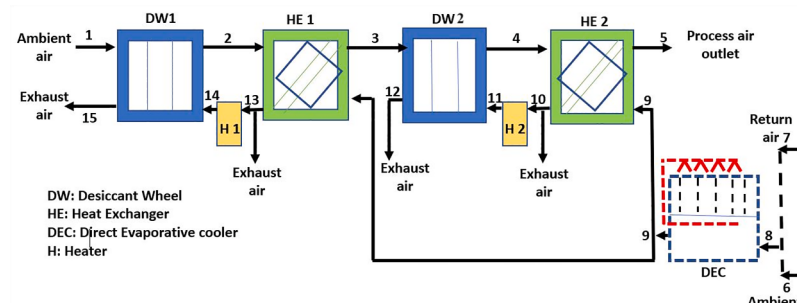
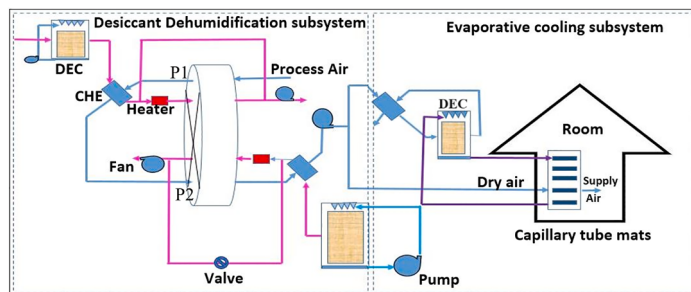


Fig. 8. Schematic diagram of two stage dehumidification and cooling system from two-rotary desiccant wheel (Ge et al., 2009).

Table 5

Research article with two desiccant wheel studies for two-stage dehumidification.

Reference	Study	Process	Material	Key finding	Energy source
(Ge et al., 2009)	Experimental	Two-stage cooling	Silica gel-haloid	This system demonstrated excellent performance with a low required regeneration temperature and a high COP. Reducing the inlet temperature and humidity ratio of the regeneration air further enhanced its efficiency.	Solar heat
(Ge et al., 2010b)	Experimental	two-stage solar-driven rotary desiccant	Silica gel-haloid composite	The optimal rotational speed for regeneration temperatures between 60 °C and 100 °C ranged from 4 to 8 rph. The system demonstrated significant advantages with a relatively high COP and a lower regeneration temperature of 68 °C, which is 28.5 % less than that of a one-stage system. Additionally, when the regeneration temperature remained constant, the system exhibited a 40 % increase in cooling capacity.	Solar heat
(La et al., 2011)	Experimental and TRNSYS simulation	two-stage desiccant cooling	–	Reducing electricity usage by approximately 22 %, 34 %, and 31 %, respectively.	Solar heat
(Li et al., 2012)	Experimental	Two-wheel two-stage desiccant cooling and heating	Composite desiccant materials	Moisture removal ranged from 9 to 12 g/kg. The supply air was in good condition at around 18 °C and 60 % relative humidity. Additionally, the system's cooling capacity varied between 16.3 and 25.6 kW, with a thermal COP of 0.97 during the cooling cycle.	Solar heat
(Tu et al., 2014)	Experimental and Mathematical	Two-wheel two stage desiccant	–	The desiccant dehumidification system's performance was significantly enhanced by drastically reducing the required regeneration temperature. At a supplied air humidity ratio of 10 g/kg, the system achieved a thermal COP of 5, demonstrating its high efficiency and energy-saving potential.	Condenser heat of heat pump
(Ge et al., 2015)	Mathematical modeling	Two-wheel two-stage desiccant modeling	Silica gel	With an increase in regeneration temperatures, the cooling capacity of the system enhanced, whereas thermal COP decreased.	–
(Tavakol and Behbahania, 2018)	Mathematical modeling	Two-wheel two-stage desiccant modeling	Silica gel	The exergy efficiency and coefficient of performance were increased by 1.12 % and 37.66 %, respectively, when compared to the conventional single-stage fresh air cycle.	–
(Asadi and Roshanzadeh, 2019)	Mathematical modeling	Two-stage desiccant cooling	–	In two regeneration configurations thermal coefficient of performance achieved was 0.72 & 0.58 and exergy efficiency was raised by 15.5 % & 21.4 %, respectively.	–

**Fig. 9.** Two-stage desiccant cooling system from a single wheel with the regenerative evaporative cooling system (Ge et al., 2008a).

application, this unnecessary heating may increase the load of the cooling unit. Thus, it can be concluded that the primary drawback of the traditional desiccant wheel is the heating of the air during dehumidification. This heating of air can be mitigated by developing a non-adiabatic desiccant wheel, such as the DCHE (Ge et al., 2010a). In the case of a conventional desiccant wheel, there is no arrangement to neutralize the carryover heat and heat of adsorption, i.e., the entire heat goes to the desiccant wall and surrounding air. But in the case of a nonadiabatic desiccant wheel, there is an arrangement of the flow of secondary fluid or coolant in the desiccant wheel, which neutralizes the heat released and somehow reduces the exit temperature of process air.

The development of the non-adiabatic desiccant wheel was started in (Kodama et al., 2005). In this work, they proposed a multi-pass rotary dehumidifier of sandwich structure with two alternate passages, one is the air passage of honeycomb zeolite blocks, and the other is secondary fluid passage channels of aluminum as shown in Fig. 12. This figure indicates that, in the secondary fluid passage, the hot water flows on the regeneration side, and cooled air flows on the adsorption side. On the other hand, in air passages (regeneration passage or dehumidification passage) atmospheric air flows on both sides to achieve regeneration or

adsorption. The flow of air in the regeneration passage is parallel to the flow of hot water, but the flow of air in the dehumidification passage is counterflow to the flow of cooled air. The hot water heats the desiccant wall and moisture removes the air passage of the regeneration side, while cooled air neutralizes the heat of adsorption of dehumidification passage and enhances the adsorption performance. The proposed system was investigated in different operating conditions of air and water, and it was compared with conventional desiccant wheels. The dehumidification ability of the multi-pass dehumidifier was 1.3 times greater than the existing desiccant wheel even with the less cross-sectional area of adsorption than the conventional wheel. In addition, the dehumidified air exit temperature of the multi-pass rotary dehumidifier was 8 °C lower than the conventional desiccant wheel which was the main feature of the proposed system. However, this wheel was not successful because of its complexity, it also required more energy to run.

Further, development started on the non-adiabatic desiccant wheel (Narayanan et al., 2013), in this work they redesigned the desiccant wheel by incorporating an additional cooling air channel to dissipate the heat of adsorption. The cooled air enters the wheel centrally as shown in Fig. 13(a), flows radially, and exits from the peripheral side of the wheel.

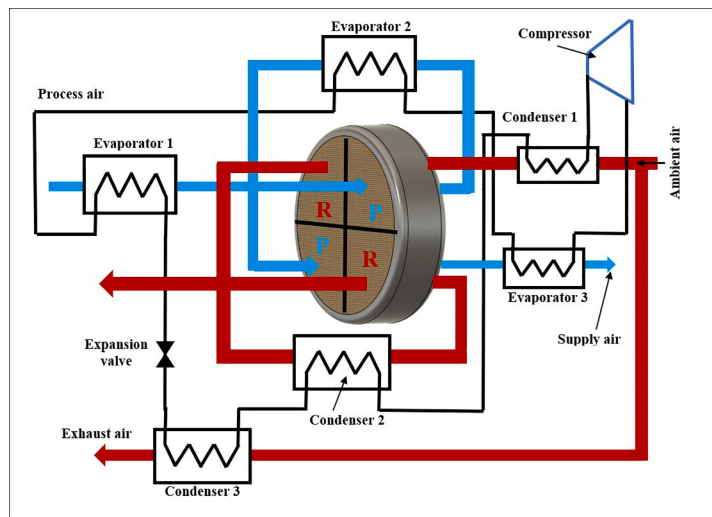


Fig. 10. Hybrid air conditioning system with four partitions desiccant wheel (Jeong et al., 2010).

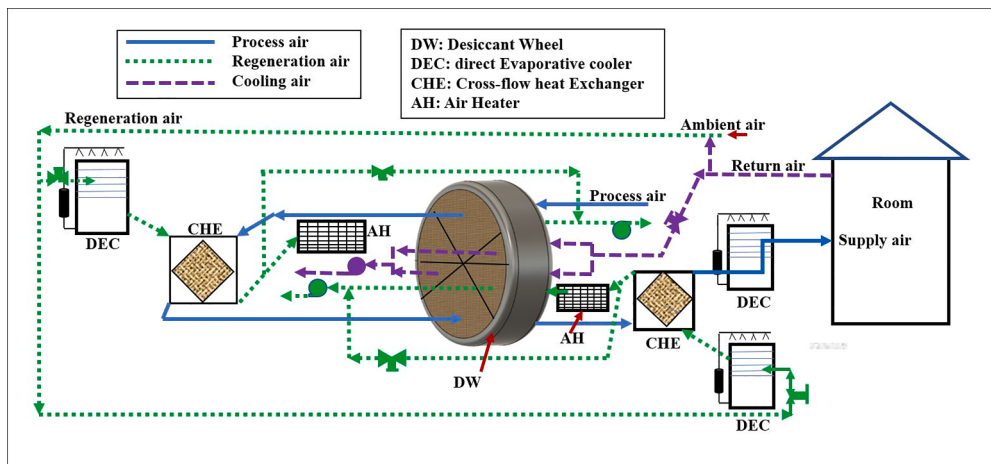


Fig. 11. Schematic diagram of solar-assisted hybrid air conditioning system with six-sector desiccant wheel (Elzahzby et al., 2014).

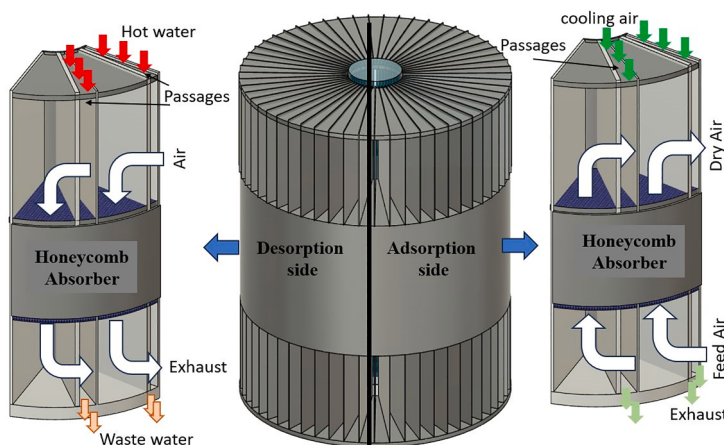


Fig. 12. Schematic diagram of air-cooled multi-pass rotary honeycomb dehumidifier regenerated by hot water (Kodama et al., 2005).

But process air flows axially in the alternate channel of the wheel, where a thin layer of desiccant is deposited as indicated in the orange color of Fig. 13(b). Their results indicated that cooled air non-adiabatic rotary wheel enhances the dehumidification by 45–53 %. However, the incorporation of an additional cooling channel reduces the

cross-sectional area for actual dehumidification.

The research on the non-adiabatic wheel was further extended by Goldsworthy and White (2014), they used water as a cooling fluid instead of air and introduced the concept of an internally water-cooled desiccant wheel as shown in Fig. 14. It is a rotary desiccant wheel but

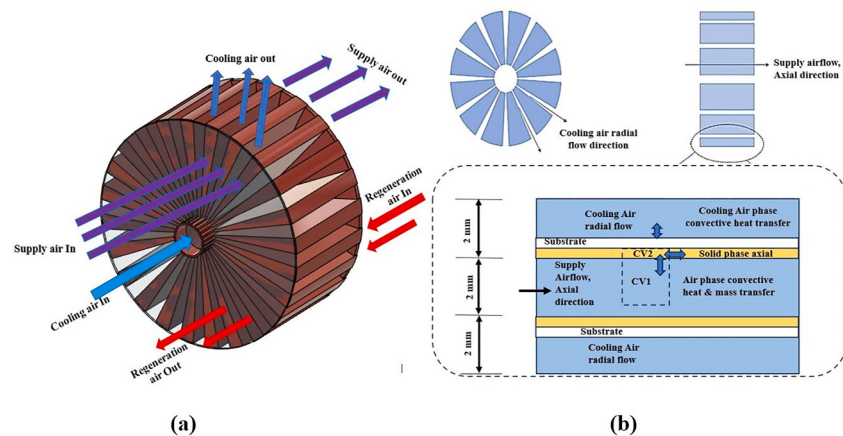


Fig. 13. (a) Non-adiabatic desiccant wheel, and (b) geometry of channel cross-section (Narayanan et al., 2013).

integrated with a shell and tube heat exchanger. The process air or regeneration air flows inside the tube of the heat exchanger in an axial direction. But cooling water enters from the central shaft of the wheel on the shell side, travels around the outer surface of tubes in the bottom half of the desiccant wheel, takes the heat of adsorption, and exits from the other end of the shell as shown on the right side of Fig. 14. The results of this study indicated that an internally cooled rotary dehumidifier offers 40 % improvement in dehumidification but with a 60 % larger diameter of the desiccant wheel for the same flow of process air as with a conventional wheel because the water channel occupies some space.

The dehumidification performance of the same wheel was further investigated in detail way by Zhou et al. (2018). The experimental setup developed by them is shown in Figs. 15(a) and 15(b). They optimized the performance of the internally cooled rotary dehumidifier and achieved isothermal dehumidification under optimum conditions as indicated in Table 6. Table 6 indicates the detailed comparison of an optimized internally cooled desiccant wheel with an existing desiccant wheel and reveals that the performance of the optimized wheel was quite better in terms of parameters shown in Table 6.

Zhou and Reece (2019) developed a non-adiabatic rotary dehumidifier with a concentric ring design as shown in Fig. 16(a) and (b) and enhanced the performance. It was made up of 14 water channels and 13 desiccant-coated channels that are sandwiched between two adjacent water channels. As shown in Fig. 16(b), water channels separate the desiccant channels from the nylon plastic wall. There is a two-axial hole on both ends of the central shaft of the wheel for water intake and outlet of the process section. Further, the side holes are used for inlet or outlet of water from the water channels as shown by a yellow arrow. The regeneration air and process air are in counterflow. Similarly, the flow of process air streams and cooling water is in counterflow which was the main feature of this novel wheel because heat exchange performance

was better in counterflow as compared to cross flow non-adiabatic desiccant wheel. The water enters from the one end of the axial hole of the shaft flows through water channels via side holes, absorbs the heat of adsorption and the carryover heat, and exits from the other end of the central hole.

The results of this study and its comparison with other types of desiccant wheels are presented in Fig. 17. It was found that the exit temperature of the supply air and humidity ratio were lower than the other type of rotary dehumidifier as shown in Fig. 17. Furthermore, it was discovered that when the difference between the inlet cooling water temperature (24°C) and process inlet temperature (25°C) of air is less (i.e., 1 K), the performance of the concentric design desiccant wheel is nearly the same as that of the traditional desiccant wheel. But when this difference increases, the dehumidification obtained with a co-centric design wheel shifts from adiabatic to isothermal dehumidification.

Recently, Zhou (2021) investigated the performance solar-driven desiccant air conditioning system by combining the internally cooled desiccant wheel with a dew point evaporative cooler at different climatic conditions. However, their conclusion indicated that the ICDW did not provide satisfactory MR in hot and humid climates when the regeneration temperature was lower than 60°C . Because the exit humidity ratio of the process stream was too high which resulted in higher wet bulb temperature, it was unable to provide adequate sensible cooling to the buildings.

The discovery of the internally cooled desiccant wheel to realize constant temperature dehumidification is one of the key successes in the usage of the desiccant wheel in HVAC but the major problem is that the size and rate of the internally cooled wheel will be higher than the existing desiccant wheel. So, more focused research is required to commercialize the desiccant wheel in HVAC applications as compared to other applications.

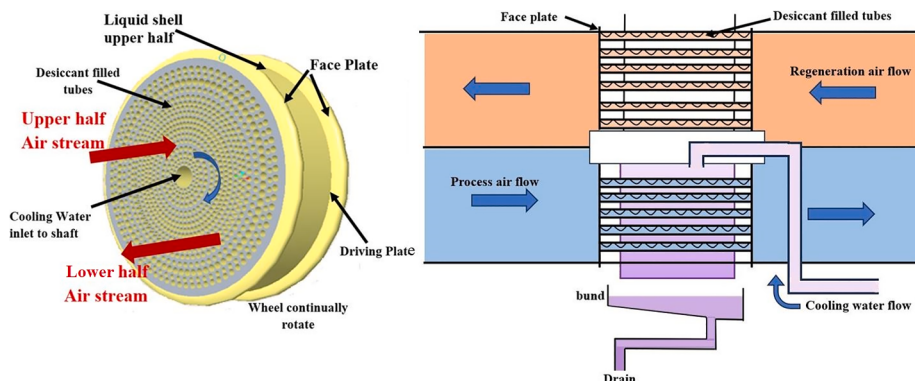


Fig. 14. 3D depiction of the internally cooled rotary dehumidifier, and cross-sectional view indicating water and air flow paths (Goldsorthy and White, 2014).

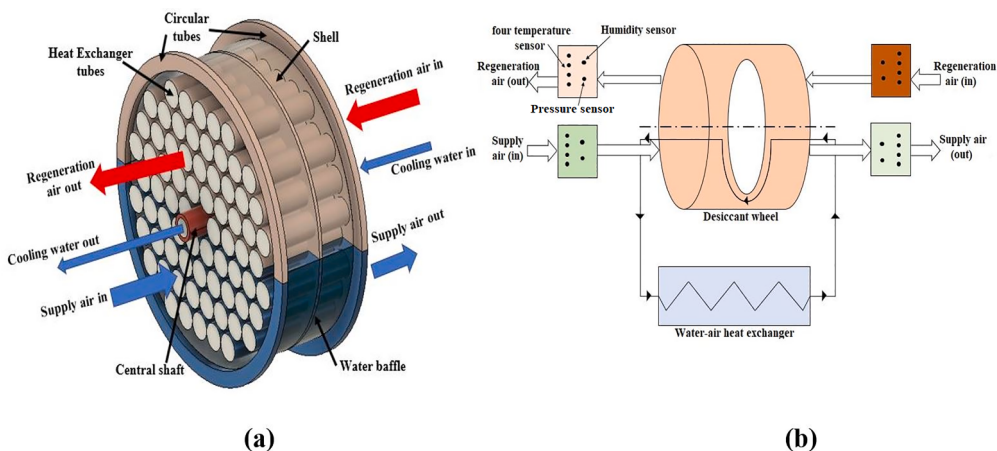


Fig. 15. (a) 3-dimensional view of an Internally cooled desiccant wheel (ICDW), (b) ICDW showing the flow of air streams and close loop of water circulation using a heat exchanger (Zhou et al., 2018).

Table 6
Desiccant wheel comparison based on air flow conditions (Zhou et al., 2018).

Airflow conditions	A system with an existing desiccant wheel	A system with optimized internally cooled DW	A system with experimentally tested DW
Exit temperature of supply air after the desiccant wheel	42 °C	30 °C	38 °C
Supply temperature of the building	24.2 °C	19.7 °C	22.8 °C
Supply humidity ratio of building	13.2 g kg ⁻¹	11.4 g kg ⁻¹	12.6 g kg ⁻¹
Specific sensible cooling capacity	6.4 kW m ⁻²	11.4 kW m ⁻²	10.4 kW m ⁻²
Total cooling capacity	13.2 kW m ⁻²	21.6 kW m ⁻²	18.4 kW m ⁻²
Specific latent cooling capacity	6.8 kW m ⁻²	10.2 kW m ⁻²	8.0 kW m ⁻²
Increase in temperature of cooling water after internally cooled desiccant wheel (ICDW)	Not applicable	1.1 K	0.95 K
Total consumption of electricity	1.7 kW	2.3 kW	2.1 kW
Energy efficiency ratio (EER)	7.7	9.3	8.1

Verma and Yadav (2023) proposed a novel four-sector rotary dehumidifier that was not internally cooled, but the objective was to reduce carryover heat and get multi-output from a single wheel. They divided the desiccant wheel into four sections and decided the optimal wheel sector angle (Regeneration 2 = 105°, Process 1 = 75°, Regeneration 1 = 120°, and Process 2 = 60°) for these four sections based on their application. They have decided the positions of these sectors and input conditions in such a manner that rotation of the wheel transfers less carryover to one of the process sections and more carryover heat to another process section as shown in below Fig. 18.

4. Conclusions

The aim of this review is to outline the significant discoveries concerning the desiccant wheel's purge section featuring multi-sector configurations, as well as novel wheel designs such as the non-adiabatic desiccant wheel. Additionally, it explores the implementation of two-stage dehumidification employing both two-sector and multi-sector (using single wheel) setups. Upon completion of the review study, the following conclusions have been drawn:

- The addition of a third small sector (purge) improves the desiccant wheel's performance. The optimal value of the purge wheel sector angle reduces not only the wheel's energy consumption but also the process air's exit temperature. As a result, there are still

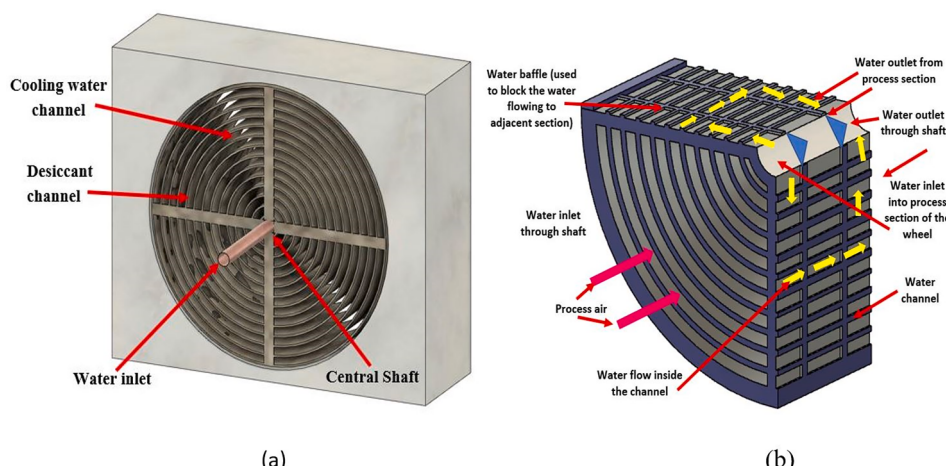


Fig. 16. (a) Non-adiabatic desiccant wheel with concentric a structure, and (b) Part of the non-adiabatic desiccant wheel showing the path of air and water flow (Zhou and Reece, 2019).

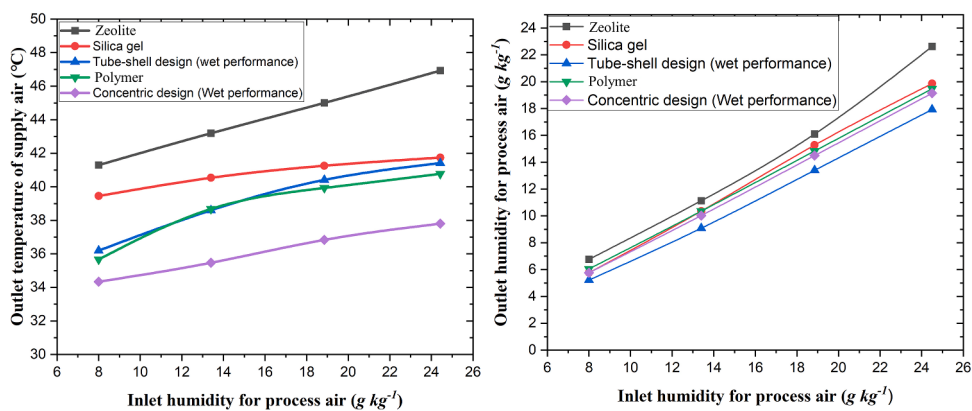


Fig. 17. Comparisons of conventional desiccant wheels (based on tube-shell and concentric designs) and internally cooled desiccant wheels (based on zeolite, silica gel, and polymer desiccant) (Zhou and Reece, 2019).

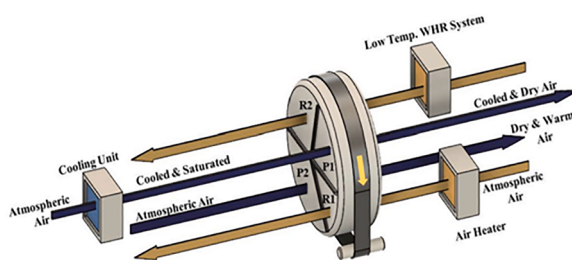


Fig. 18. Novel four sector rotary dehumidifier configurations for optimization of carryover heat into P1 and P2 (Verma and Yadav, 2023).

opportunities to enhance the desiccant wheel's overall performance by focusing on the purge and its parameters.

- The non-adiabatic desiccant wheel presented by researchers reduces the exit temperature of the desiccant wheel and achieves isothermal dehumidification. But with the introduction of secondary cooling fluid the complexity of the wheel increases. Hence, there is a still need to develop some novel designs for desiccant wheels which can reduce the exit temperature and make the wheel simple and easy to operate.
- Two-stage dehumidification using a single wheel with multi-sector is one of the suitable options to get multi-output from a single wheel. In the multi-sector wheel, we can provide cooling from one section by introducing a cooling section before or after wheel sections, and from the remaining sections dry, humid, and hot air. Hence, several investigations can also be carried out on the multi-sector desiccant wheel to get two-stage dehumidification and to get cooling and drying from a single wheel.

Funding

This research did not receive any specific grant from funding agencies in the public, commercial, or not-for-profit sectors.

CRedit authorship contribution statement

Laxmikant Yadav: Writing – review & editing, Writing – original draft, Validation, Supervision, Software, Resources, Methodology, Investigation, Formal analysis, Conceptualization. **Ashutosh Kumar Verma:** Visualization, Software, Resources, Data curation, Formal analysis, Investigation.

Declaration of competing interest

The authors declare that they have no known competing financial

interests or personal relationships that could have appeared to influence the work reported in this paper.

References

- Abd-Elyadhy, M.M., Salem, M.S., Hamed, A.M., El-Sharkawy, I.I., 2022. Solid desiccant-based dehumidification systems: a critical review on configurations, techniques, and current trends. *Int. J. Refrig.* 133, 337–352. <https://doi.org/10.1016/j.ijrefrig.2021.09.028>.
- Abdelgaidi, M., Saber, M.A., Bassuoni, M.M., Khaira, A.M., 2023. Solid desiccant air conditioning system using desiccant dehumidifiers with cooling technique and thermal recovery unit: experimental investigation and performance analysis. *J. Clean. Prod.* 421, 138387 <https://doi.org/10.1016/j.jclepro.2023.138387>.
- Ahmed, M.H., Kattab, N.M., Fouad, M., 2005. Evaluation and optimization of solar desiccant wheel performance. *Renew. Energy* 30, 305–325. <https://doi.org/10.1016/j.renene.2004.04.010>.
- Akhtar, M.U.S., Fadlallah, S.O., Khan, M.I., Asfand, F., Al-Ghamdi, S.G., Mishra, R., 2024. Sustainable humidity control in the built environment: recent research and technological advancements in thermal driven dehumidification systems. *Energy Build* 304, 113846. <https://doi.org/10.1016/j.enbuild.2023.113846>.
- Al-Shetwi, A.Q., 2022. Sustainable development of renewable energy integrated power sector: trends, environmental impacts, and recent challenges. *Sci. Total Environ.* 822, 153645 <https://doi.org/10.1016/j.scitotenv.2022.153645>.
- Angrisani, G., Diglio, G., Sasso, M., Calise, F., Dentice d'Accademia, M., 2016. Design of a novel geothermal heating and cooling system: energy and economic analysis. *Energy Convers. Manag.* 108, 144–159. <https://doi.org/10.1016/j.enconman.2015.11.001>.
- Angrisani, G., Minichiello, F., Roselli, C., Sasso, M., 2012. Experimental analysis on the dehumidification and thermal performance of a desiccant wheel. *Appl. Energy* 92, 563–572. <https://doi.org/10.1016/j.apenergy.2011.11.071>.
- Asadi, A., Roshanzadeh, B., 2019. Improving performance of two-stage desiccant cooling system by analyzing different regeneration configurations. *J. Build. Eng.* 25, 100807 <https://doi.org/10.1016/j.jobr.2019.100807>.
- ASHRAE, 1974. Symposium on heat recovery. *ASHRAE Trans* 80 (1), 302–332.
- Bharathi, A.L.K., Hussain, S.I., Kalaiselvam, S., 2023. Performance evaluation of various fiber paper matrix desiccant wheels coated with nano-adsorbent for energy efficient dehumidification. *Int. J. Refrig.* 146, 416–429. <https://doi.org/10.1016/j.ijrefrig.2022.12.002>.
- Buker, M.S., Parlamic, H.I., Alwetaishi, M., Benjedou, O., 2022. Experimental investigation on the dehumidification performance of a parabolic trough solar air collector assisted rotary desiccant system. *Case Stud. Therm. Eng.* 34 <https://doi.org/10.1016/j.csite.2022.102077>.
- Cerci, K.N., Hurdogan, E., 2022. Performance assessment of a heat pump assisted rotary desiccant dryer for low temperature peanut drying. *Biosyst. Eng.* 223, 1–17. <https://doi.org/10.1016/jbiosystemseng.2022.08.009>.
- Chen, Q., Jones, J.R., Archer, R.H., 2019. A dehumidification process with cascading desiccant wheels to produce air with dew point below 0 °C. *Appl. Therm. Eng.* 148, 78–86. <https://doi.org/10.1016/j.applthermaleng.2018.10.114>.
- Chen, X., Riffat, S., Bai, H., Zheng, X., Reay, D., 2020. Recent progress in liquid desiccant dehumidification and air-conditioning: a review. *Energy Built Environ.* 1, 106–130. <https://doi.org/10.1016/j.enbenv.2019.09.001>.
- Chung, J.Y., Park, M.H., Hong, S.H., Baek, J., Han, C., Lee, S., Kang, Y.T., Kim, Y., 2023. Comparative performance evaluation of multi-objective optimized desiccant wheels coated with MIL-100 (Fe) and silica gel composite. *Energy* 283, 128567. <https://doi.org/10.1016/j.energy.2023.128567>.
- DAC, 2022. Energy Recovery wheel [WWW Document]. www.dac-hvac.com. URL <http://www.dac-hvac.com/wp-content/uploads/Energy-Recovery-Wheel-Purge.pdf> (accessed 12.23.22).
- Dai, Y., Li, X., Wang, R., 2015. Theoretical analysis and case study on solar driven two-stage rotary desiccant cooling system combined with geothermal heat pump. *Energy Procedia* 70, 418–426. <https://doi.org/10.1016/j.egypro.2015.02.143>.

- Daou, K., Wang, R.Z., Xia, Z.Z., 2006. Desiccant cooling air conditioning: a review. *Renew. Sustain. Energy Rev.* 10, 55–77. <https://doi.org/10.1016/j.rser.2004.09.010>.
- De Antonellis, S., Joppolo, C.M., Molinaroli, L., 2010. Simulation, performance analysis and optimization of desiccant wheels. *Energy Build.* 42, 1386–1393. <https://doi.org/10.1016/j.enbuild.2010.03.007>.
- Dincer, I.M.A.R., 2007. Exergy analysis of psychrometric processes. Exergy energy. *Environ. Sustain. Dev.* <https://doi.org/10.1016/B978-008044529-8.50009-4>.
- Dunkle, R., 1965. A methods of solar air conditioning. *Mech. Chem. Eng. Trans.* 01, 73–78.
- Ebrahimi, M., Keshavarz, A., 2015. CCHP Technology. *Comb. Cool. Heat. Power* 35–91. <https://doi.org/10.1016/b978-0-08-099985-2.00002-0>.
- El-Agouz, S.A., Kabel, A.E., 2014. Performance of desiccant air conditioning system with geothermal energy under different climatic conditions. *Energy Convers. Manag.* 88, 464–475. <https://doi.org/10.1016/j.enconman.2014.08.027>.
- Elsarrag, E., Igboho, O.N., Alhorri, Y., Davies, P.A., 2016. Solar pond powered liquid desiccant evaporative cooling. *Renew. Sustain. Energy Rev.* 58, 124–140. <https://doi.org/10.1016/j.rser.2015.12.053>.
- Elzahby, A.M., Kabel, A.E., Bassouoni, M.M., Abdelaied, M., 2014. A mathematical model for predicting the performance of the solar energy assisted hybrid air conditioning system, with one-rotor six-stage rotary desiccant cooling system. *Energy Convers. Manag.* 77, 129–142. <https://doi.org/10.1016/j.enconman.2013.08.052>.
- Faroog, S., Ruthven, D.M., 1991. Numerical simulation of a desiccant bed for solar air conditioning applications. *J. Sol. Energy Eng. Trans. ASME* 113, 80–88. <https://doi.org/10.1115/1.2929962>.
- Feng, Y.H., Dai, Y.J., Wang, R.Z., Ge, T.S., 2022. Insights into desiccant-based internally-cooled dehumidification using porous sorbents: from a modeling viewpoint. *Appl. Energy* 311. <https://doi.org/10.1016/j.apenergy.2022.118732>.
- Ge, T.S., Dai, Y.J., Wang, R.Z., 2014. Review on solar powered rotary desiccant wheel cooling system. *Renew. Sustain. Energy Rev.* 39, 476–497. <https://doi.org/10.1016/j.rser.2014.07.121>.
- Ge, T.S., Dai, Y.J., Wang, R.Z., Li, Y., 2015. Performance of two-stage rotary desiccant cooling system with different regeneration temperatures. *Energy* 80, 556–566. <https://doi.org/10.1016/j.energy.2014.12.010>.
- Ge, T.S., Dai, Y.J., Wang, R.Z., Li, Y., 2008a. Experimental investigation on a one-rotor two-stage rotary desiccant cooling system. *Energy* 33, 1807–1815. <https://doi.org/10.1016/j.energy.2008.08.006>.
- Ge, T.S., Dai, Y.J., Wang, R.Z., Peng, Z.Z., 2010a. Experimental comparison and analysis on silica gel and polymer coated fin-tube heat exchangers. *Energy* 35, 2893–2900. <https://doi.org/10.1016/j.energy.2010.03.020>.
- Ge, T.S., Li, Y., Dai, Y.J., Wang, R.Z., 2010b. Performance investigation on a novel two-stage solar driven rotary desiccant cooling system using composite desiccant materials. *Sol. Energy* 84, 157–159. <https://doi.org/10.1016/j.solener.2009.12.008>.
- Ge, T.S., Li, Y., Wang, R.Z., Dai, Y.J., 2009. Experimental study on a two-stage rotary desiccant cooling system. *Int. J. Refrig.* 32, 498–508. <https://doi.org/10.1016/j.ijrefrig.2008.07.001>.
- Ge, T.S., Li, Y., Wang, R.Z.A., Dai, Y.J., 2008b. A review of the mathematical models for predicting rotary desiccant wheel. *Renew. Sustain. Energy Rev.* 12, 1485–1528. <https://doi.org/10.1016/j.rser.2007.01.012>.
- Ge, T.S., Ziegler, F., Wang, R.Z., 2010c. A mathematical model for predicting the performance of a compound desiccant wheel (A model of compound desiccant wheel). *Appl. Therm. Eng.* 30, 1005–1015. <https://doi.org/10.1016/j.aplthermaleng.2010.01.012>.
- Goldsworthy, M.J., White, S., 2014. Design and performance of an internal heat exchange desiccant wheel. *Int. J. Refrig.* 39, 152–159. <https://doi.org/10.1016/j.ijrefrig.2013.10.009>.
- Golubovic, M.N., Hettiarachchi, H.D.M., Worek, W.M., 2007. Evaluation of rotary dehumidifier performance with and without heated purge. *Int. Commun. Heat Mass Transf* 34, 785–795. <https://doi.org/10.1016/j.icheatmastransfer.2007.03.011>.
- Harshe, Y.M., Utikar, R.P., Ranade, V.V., Pahwa, D., 2005. Modeling of rotary desiccant wheels. *Chem. Eng. Technol.* 28, 1473–1479. <https://doi.org/10.1002/ceat.200500164>.
- Herath, H.M.D.P., Wickramasinghe, M.D.A., Polgolla, A.M.C.K., Jayasena, A.S., Ranasinghe, R.A.C.P., Wijewardane, M.A., 2020. Applicability of rotary thermal wheels to hot and humid climates. *Energy Rep.* 6, 539–544. <https://doi.org/10.1016/j.egyr.2019.11.116>.
- IEA, 2022. Space Cooling Report [WWW Document]. www.iea.org. URL. <https://www.iea.org/reports/space-cooling>.
- Intini, M., Goldsworthy, M., White, S., Joppolo, C.M., 2015. Experimental analysis and numerical modelling of an AQSOA zeolite desiccant wheel. *Appl. Therm. Eng.* 80, 20–30. <https://doi.org/10.1016/j.aplthermaleng.2015.01.036>.
- Jani, D.B., Mishra, M., Sahoo, P.K., 2018. A critical review on application of solar energy as renewable regeneration heat source in solid desiccant – vapor compression hybrid cooling system. *J. Build. Eng.* 18, 107–124. <https://doi.org/10.1016/j.jobe.2018.03.012>.
- Jani, D.B., Mishra, M., Sahoo, P.K., 2016. Solid desiccant air conditioning - a state of the art review. *Renew. Sustain. Energy Rev.* 60, 1451–1469. <https://doi.org/10.1016/j.rser.2016.03.031>.
- Jeong, J., Yamaguchi, S., Saito, K., Kawai, S., 2010. Performance analysis of four-partition desiccant wheel and hybrid dehumidification air-conditioning system. *Int. J. Refrig.* 33, 496–509. <https://doi.org/10.1016/j.ijrefrig.2009.12.001>.
- Kashif, A., Ali, M., Sheikh, N.A., Vukovic, V., Shehryar, M., 2020. Experimental analysis of a solar assisted desiccant-based space heating and humidification system for cold and dry climates. *Appl. Therm. Eng.* 175. <https://doi.org/10.1016/j.aplthermaleng.2020.115371>.
- Kodama, A., Watanabe, N., Hirose, T., Goto, M., Okano, H., 2005. Performance of a multipass honeycomb adsorber regenerated by a direct hot water heating. *Adsorption* 11, 603–608. <https://doi.org/10.1007/s10450-005-5992-6>.
- La, D., Dai, Y., Li, Y., Ge, T., Wang, R., 2011. Case study and theoretical analysis of a solar driven two-stage rotary desiccant cooling system assisted by vapor compression air-conditioning. *Sol. Energy* 85, 2997–3009. <https://doi.org/10.1016/j.solener.2011.08.039>.
- La, D., Dai, Y.J., Li, Y., Ge, T.S., Wang, R.Z., 2012. Use of regenerative evaporative cooling to improve the performance of a novel one-rotor two-stage solar desiccant dehumidification unit. *Appl. Therm. Eng.* 42, 11–17. <https://doi.org/10.1016/j.aplthermaleng.2011.01.010>.
- La, D., Dai, Y.J., Li, Y., Wang, R.Z., Ge, T.S., 2010. Technical development of rotary desiccant dehumidification and air conditioning: a review. *Renew. Sustain. Energy Rev.* <https://doi.org/10.1016/j.rser.2009.07.016>.
- Li, H., Dai, Y.J., Li, Y., La, D., Wang, R.Z., 2012. Case study of a two-stage rotary desiccant cooling/heating system driven by evacuated glass tube solar air collectors. *Energy Build* 47, 107–112. <https://doi.org/10.1016/j.enbuild.2011.11.035>.
- Liu, Z., Cheng, C., Han, J., Zhao, Z., Qi, X., 2022. Experimental evaluation of the dehumidification performance of a metal organic framework desiccant wheel. *Int. J. Refrig.* 133, 157–164. <https://doi.org/10.1016/j.ijrefrig.2021.09.033>.
- Ma, Z., Chang, X., Zhang, T., Liu, X., Guan, B., 2024. On-site measurement and optimization of energy efficiency of the cascading desiccant wheel deep dehumidification systems in the lithium-ion battery manufacturing factory. *Energy Build* 304, 113833. <https://doi.org/10.1016/j.enbuild.2023.113833>.
- Majumdar, P., 1998. Heat and mass transfer in composite desiccant pore structures for dehumidification. *Sol. Energy* 62, 1–10.
- Mandegari, M.A., Farzad, S., Angrisani, G., Pahlavanzadeh, H., 2017. Study of purge angle effects on the desiccant wheel performance. *Energy Convers. Manag.* 137, 12–20. <https://doi.org/10.1016/j.enconman.2017.01.042>.
- Mazzei, P., Minichiello, F., Palma, D., 2005. HVAC dehumidification systems for thermal comfort: a critical review. *Appl. Therm. Eng.* 25, 677–707. <https://doi.org/10.1016/j.aplthermaleng.2004.07.014>.
- Mei, V.C., Chen, F.C., Lavan, Z., Collier, R.K., Meckler, G., 1992. An Assessment of Desiccant Cooling and Dehumidification Technology, pp. 1–108. Prepared by the OAK Ridge National Laboratory, Tennessee 37831-6285 managed by Martin Marietta Energy System, Inc. for the US Department of Energy under Contract No. DE-AC05-84OR21400.
- Ministry of New and Renewable Energy, 2010. Ministry of new and renewable energy - resolution.
- Mohammed, R.H., Ahmadi, M., Ma, H., Bigham, S., 2023. Desiccants enabling energy-efficient buildings: a review. *Renew. Sustain. Energy Rev.* 183, 113418. <https://doi.org/10.1016/j.rser.2023.113418>.
- Motaghian, S., Pasdarshahi, H., 2020. Regeneration energy analysis and optimization in desiccant wheels using purge mechanism. *J. Build. Eng.* 27, 100980. <https://doi.org/10.1016/j.jobe.2019.100980>.
- Motaghian, S., Rayegan, S., Pasdarshahi, H., Ahmadi, P., Rosen, M.A., 2021. Comprehensive performance assessment of a solid desiccant wheel using an artificial neural network approach. *Int. J. Heat Mass Transf.* 165, 120657. <https://doi.org/10.1016/j.icheatmastransfer.2020.120657>.
- Mujahid Rafique, M., Gandhidasan, P., Rehman, S., Al-Hadhrami, L.M., 2015. A review on desiccant based evaporative cooling systems. *Renew. Sustain. Energy Rev.* 45, 145–159. <https://doi.org/10.1016/j.rser.2015.01.051>.
- Munter, C., 1968. Inorganic, fibrous, gas conditioning packing for heat and moisture transfer.
- munters, 2022. Desiccant Roater Industrial Dehumidification [WWW Document]. www.munters.com. URL. <https://www.munters.com/en/about-us/history-of-munters/history-news/muntersdesiccant-rotor-industrial-dehumidification-at-its-best/> (accessed 12.23.22).
- Nagaya, K., Li, Y., Jin, Z., Fukumuro, M., Ando, Y., Akaishi, A., 2006. Low-temperature desiccant-based food drying system with airflow and temperature control. *J. Food Eng.* 75, 71–77. <https://doi.org/10.1016/j.jfoodeng.2005.03.051>.
- Narayanan, R., Saman, W.Y., White, S.D., 2013. A non-adiabatic desiccant wheel: modeling and experimental validation. *Appl. Therm. Eng.* 61, 178–185. <https://doi.org/10.1016/j.aplthermaleng.2013.07.007>.
- Pennington N.A., 1955. 47U2700537.
- Pesaran, A.A., Penney, T.R., Czanderna, W., 1992. Desiccant Cool : State-of-the-Art ; sessment 11.
- Rambhad, K.S., Walke, P.V., Tidke, D.J., 2016. Solid desiccant dehumidification and regeneration methods - a review. *Renew. Sustain. Energy Rev.* 59, 73–83. <https://doi.org/10.1016/j.rser.2015.12.264>.
- Robison, H.I., 1985. Passive and low-energy research and practices - dehumidification, Passive and low energy ecotechniques. In: Proc. 3rd PLEA conference. Pergamon Press Ltd, Mexico City. <https://doi.org/10.1016/b978-0-08-031644-4.50011-4>, 1984.
- Ruan, W., Qu, M., Horton, W.T., 2012. Modeling analysis of an enthalpy recovery wheel with purge air. *Int. J. Heat Mass Transf.* 55, 4665–4672. <https://doi.org/10.1016/j.ijheatmasstransfer.2012.04.025>.
- San, J.Y., 1988. The effects of desiccant content and purging process on the performance of a rotary desiccant cooling system. *J. Chinese Inst. Eng. Trans. Chinese Inst. Eng. A/Chung-kuo K. Ch'eng Hsueh K'an* 11, 385–390. <https://doi.org/10.1080/02533839.1988.9677084>.
- Seckin Salvarli, M., Salvarli, H., 2020. For sustainable development: future trends in renewable energy and enabling technologies. *Renew. Energy - Resour. Chall. Appl.* 1–15. <https://doi.org/10.5772/intechopen.91842>.
- Shamim, J.A., Hsu, W.L., Paul, S., Yu, L., Daigui, H., 2021. A review of solid desiccant dehumidifiers: current status and near-term development goals in the context of net

- zero energy buildings. *Renew. Sustain. Energy Rev.* 137, 110456 <https://doi.org/10.1016/j.rser.2020.110456>.
- Su, M., Han, X., Chang, H., Chong, D., Liu, J., Yan, J., 2023. Performance investigation and exergy analysis of a novel recirculated regenerative solid desiccant dehumidification system. *J. Build. Eng.* 67, 106029 <https://doi.org/10.1016/j.jobe.2023.106029>.
- Sultan, M., El-Sharkawy, I.I., Miyazaki, T., Saha, B.B., Koyama, S., 2015. An overview of solid desiccant dehumidification and air conditioning systems. *Renew. Sustain. Energy Rev.* 46, 16–29. <https://doi.org/10.1016/j.rser.2015.02.038>.
- Tavakol, P., Behbahaninia, A., 2018. Presentation of two new two-stage desiccant cooling cycles based on heat recovery and evaluation of performance based on energy and exergy analysis. *J. Build. Eng.* 20, 455–466. <https://doi.org/10.1016/j.jobe.2018.08.002>.
- Tian, S., Su, X., Geng, Y., 2022. Review on heat pump coupled desiccant wheel dehumidification and air conditioning systems in buildings. *J. Build. Eng.* 54, 104655 <https://doi.org/10.1016/j.jobe.2022.104655>.
- Tu, R., Liu, X.H., Jiang, Y., 2014. Performance analysis of a two-stage desiccant cooling system. *Appl. Energy* 113, 1562–1574. <https://doi.org/10.1016/j.apenergy.2013.09.016>.
- Verma, A.K., Yadav, L., 2023. Investigation of angular aspects of a novel four-sector rotary dehumidifier configuration for HVAC applications. *J. Build. Eng.* 71, 106490 <https://doi.org/10.1016/j.jobe.2023.106490>.
- Verma, A.K., Yadav, L., Agrawal, D., Dhamija, A., Rajneesh, Bijalwan, G., 2022. Mathematical investigation of two-stage dehumidification from single rotary dehumidifier with and without precooling. *Numer. Heat Transf. Part A Appl.* 82, 82–108. <https://doi.org/10.1080/10407782.2022.2066922>.
- Vivekh, P., Pei, S.D., Pang, W., Cheng, G., 2023. Air dehumidification performance study of a desiccant wheel by a three-dimensional mathematical model. *Int. J. Refrig.* 147, 163–173. <https://doi.org/10.1016/j.ijrefrig.2022.10.011>.
- Worke, W.M., Choudhuri, K., 1982. Hybrid desiccant vapor compression cooling system. *Southeastern Seminar On Thermal Sciences. 16/1981, MIAMI USA*, pp. 156–157.
- Wu, X.N., Ge, T.S., Dai, Y.J., Wang, R.Z., 2018. Review on substrate of solid desiccant dehumidification system. *Renew. Sustain. Energy Rev.* 82, 3236–3249. <https://doi.org/10.1016/j.rser.2017.10.021>.
- Xue, Y., Li, Q., Wang, R., Ge, T., 2024. Performance analysis of a rotary desiccant wheel using polymer material with high water uptake and low regeneration temperature. *Int. J. Refrig.* 158, 385–392. <https://doi.org/10.1016/j.ijrefrig.2023.12.003>.
- Yadav, A., Bajpai, V., 2013. Analysis of various designs of a desiccant wheel for improving the performance using a mathematical model. *J. Renew. Sustain. Energy* 5. <https://doi.org/10.1063/1.4794748>.
- Yadav, A., 2014. Analysis of desiccant wheel with purge sector for improving the performance using a mathematical model. *Int. J. Air-Condition. Refrig.* 22, 1450004 <https://doi.org/10.1142/s2010132514500047>.
- Yadav, A., Bajpai, V.K., 2012. Mathematical model for design parameter analysis to improve the performance of a desiccant wheel. *Chem. Eng. Technol.* 35, 1617–1625. <https://doi.org/10.1002/ceat.201100536>.
- Yadav, A., Yadav, L., 2015. Comparative Performance of Different Sector Arrangement in a Desiccant Wheel Using a Mathematical Model. *Heat Transf. - Asian Res.* 44, 133–153. <https://doi.org/10.1002/htj.21103>.
- Yadav, A., Yadav, L., 2014. Comparative performance of desiccant wheel with effective and ordinary regeneration sector using mathematical model. *Heat Mass Transf. und Stoffuebertragung* 50, 1465–1478. <https://doi.org/10.1007/s00231-014-1349-6>.
- Yadav, L., Yadav, A., 2018a. Parametric analysis of desiccant wheel for air conditioning application. *Heat Transf. - Asian Res.* 47, 771–793. <https://doi.org/10.1002/htj.21338>.
- Yadav, L., Yadav, A., 2018b. Effect of different arrangements of sector on the performance of desiccant wheel. *Heat Mass Transf. und Stoffuebertragung* 54, 7–23. <https://doi.org/10.1007/s00231-017-2092-6>.
- Yadav, L., Yadav, A., 2016. Mathematical investigation of purge sector angle for clockwise and anticlockwise rotation of desiccant wheel. *Appl. Therm. Eng.* 93, 839–848. <https://doi.org/10.1016/j.applthermaleng.2015.10.062>.
- Yang, B., Wang, C., Ji, X., Nie, J., Zhang, R., Li, Y., Chen, Q., 2024. A solar-assisted regenerative desiccant air conditioning with indirect evaporative cooling for humid climate region. *Appl. Therm. Eng.* 243 <https://doi.org/10.1016/j.applthermaleng.2024.122598>.
- Yin, H., Yin, Y., 2021. Current status and development trend of dehumidification technology in low-humidity industries. *IOP Conf. Ser. Earth Environ. Sci.* 1011 <https://doi.org/10.1088/1755-1315/1011/1/012030>.
- Zeng, D.Q., Li, H., Dai, Y.J., Xie, A.X., 2014. Numerical analysis and optimization of a solar hybrid one-rotor two-stage desiccant cooling and heating system. *Appl. Therm. Eng.* 73, 474–483. <https://doi.org/10.1016/j.applthermaleng.2014.07.076>.
- Zhai, C., Archer, D.H., Fischer, J.C., 2009. Performance modeling of desiccant wheels (1): model development. In: 2008 Proc. 2nd Int. Conf. Energy Sustain. ES, 2, pp. 209–219. <https://doi.org/10.1115/es2008-54185>, 2008.
- Zhang, L.Z., Fu, H.X., Yang, Q.R., Xu, J.C., 2014. Performance comparisons of honeycomb-type adsorbent beds (wheels) for air dehumidification with various desiccant wall materials. *Energy* 65, 430–440. <https://doi.org/10.1016/j.energy.2013.11.042>.
- Zhang, Q., Li, Y., Zhang, Qiuyue, Ma, F., Lü, X., 2024a. Application of deep dehumidification technology in low-humidity industry: a review. *Renew. Sustain. Energy Rev.* 193, 114278 <https://doi.org/10.1016/j.rser.2024.114278>.
- Zhang, Y., Wang, W., Zheng, X., Cai, J., 2024b. Recent progress on composite desiccants for adsorption-based dehumidification. *Energy* 302, 131824. <https://doi.org/10.1016/j.energy.2024.131824>.
- Zhou, X., 2021. Thermal and energy performance of a solar-driven desiccant cooling system using an internally cooled desiccant wheel in various climate conditions. *Appl. Therm. Eng.* 185, 116077 <https://doi.org/10.1016/j.applthermaleng.2020.116077>.
- Zhou, X., Goldsworthy, M., Sproul, A., 2018. Performance investigation of an internally cooled desiccant wheel. *Appl. Energy* 224, 382–397. <https://doi.org/10.1016/j.applenergy.2018.05.011>.
- Zhou, X., Reece, R., 2019. Experimental investigation for a non-adiabatic desiccant wheel with a concentric structure at low regeneration temperatures. *Energy Convers. Manag.* 201, 112165 <https://doi.org/10.1016/j.enconman.2019.112165>.